Monte Carlo Predictions of Radiation Damage in the ISIS TS1 Target and Indirect Experimental Benchmarking

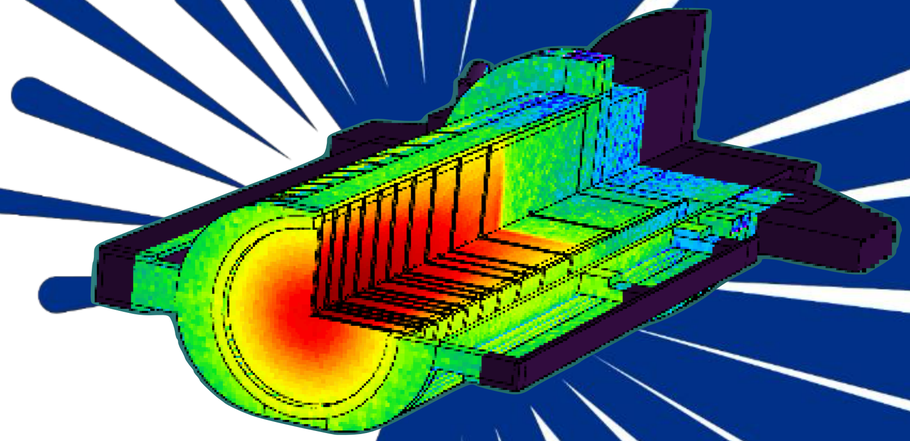

L. Quintieri[1], F. Cerutti[2], F. Salvat-Pujol[2], V. Vlachoudis[2], D.J.S. Findlay[1], D. Wilcox[1], S. Lilley[1], S.D. Gallimore[1], P. Harrison[1], D.M. Jenkins[1], C. Densham[1], P. Loveridge[1], W. Calvo[1], L. Jones[1], D. Cross[1], G.D. Howells[1], J.D. Moor[1], J. Chapman[1], J. Bryan[1], M. Jeremy[1]

[1] ISIS Neutron and Muon Source, STFC, UK
[2] CERN, Switzerland

ICANS XXV, Malmö, Sweden 16th April 2026

Science and Technology Facilities Council
ISIS Neutron and Muon Source

Overview

This talk describes the FLUKA simulations to estimate the radiation damage in ISIS TS1

- General introduction on radiation damage models in FLUKA code
  - DPA estimates: NRT and ARC-dpa
  - Average vs Peak DPA
- Description of FLUKA model of the TS1-TRAM
- FLUKA results for ISIS TS1: DPA and gas production (H and He) plate by plate estimation
- Benchmarking the FLUKA prediction by measuring temperatures profile in 2 irradiation (low and high irradiation) scenarios

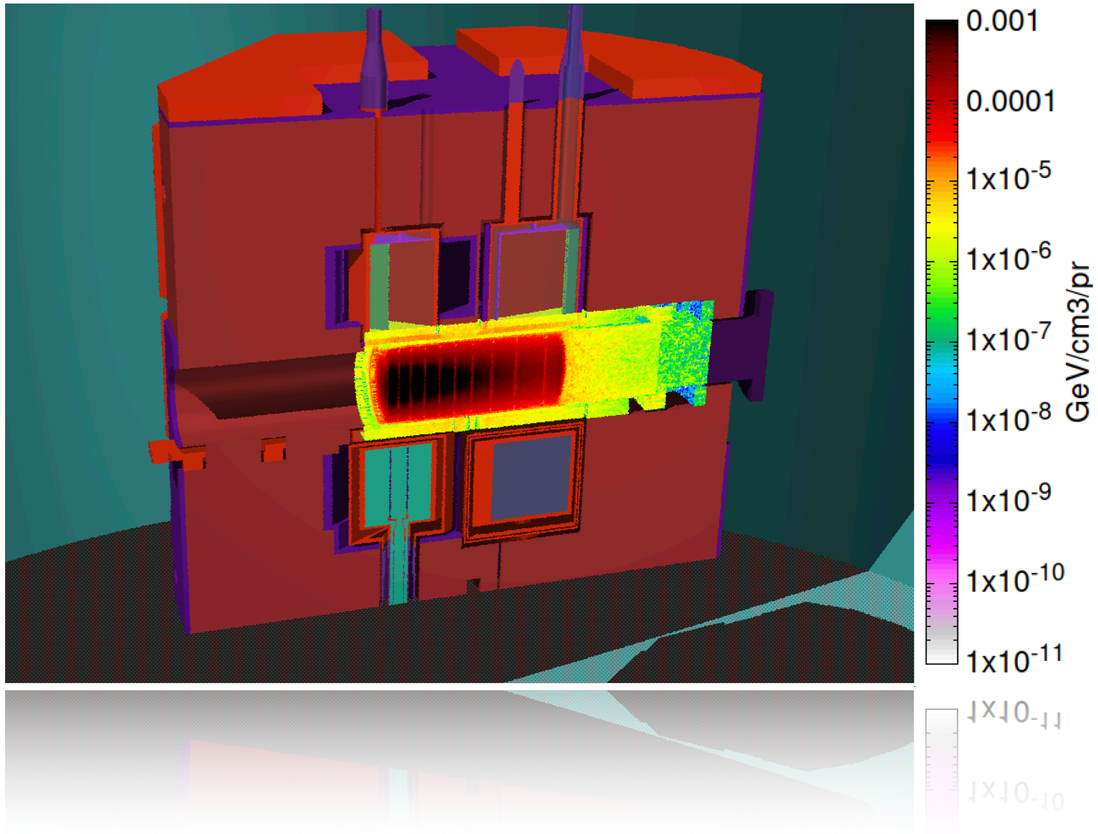

Science and Technology Facilities Council

ISIS Neutron and Muon Source

Why FLUKA?

- FLUKA is a Monte Carlo code capable of simulating the **transport of elementary particles and ions** in complex geometries and materials.
- It allows to estimate **prompt energy deposition and secondary particles production and interactions**
- Within the same input it is possible to carry out **decay heat calculation and radioactivity calculation as function of time** (no need to couple FLUKA with different codes to follow the evolution of the Radionuclei Inventory as a function of time)
- **All the decay products can be explicitly transported** within FLUKA (alpha, beta, gamma, e-, e+)
- **Radiation damage** (DPA, gas production, etc.) is enabled with advanced upgraded models (dpa-NRT, acrc-DPA)

FLUKA handles the transport+interaction of:

Photons	Leptons	Hadrons	Ions
	$e^{\pm}$, $\mu^{\pm}$, $\tau^{\pm}$ ν_X, $\bar{\nu}_X$	π^*, K^*, p, $\bar{p}$, n, $\bar{n}$, Λ, ...	${}^{A}_{Z}X$

from the keV to the PeV
(γ down to 100 eV)
(n down to 0.01 meV)

Ta+W Direct beam:

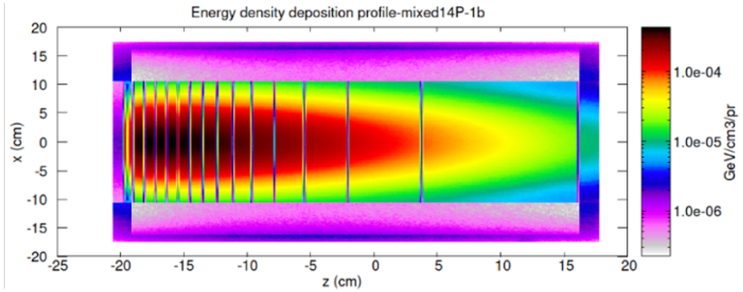

Ta+W Decay heat:

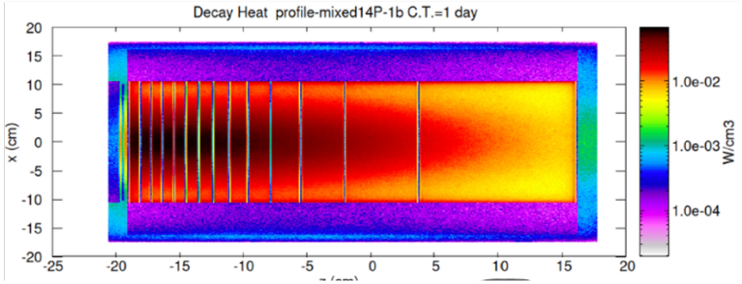

dpa distribution

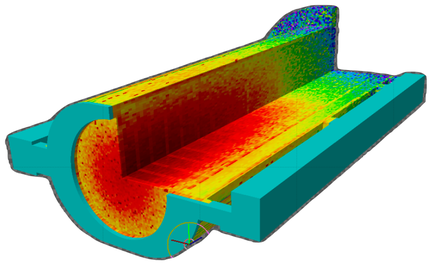

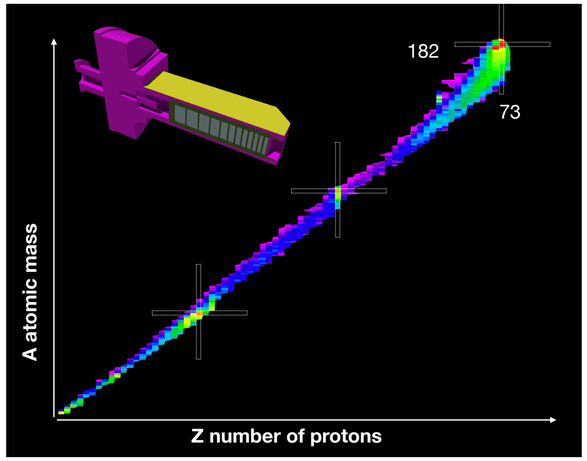

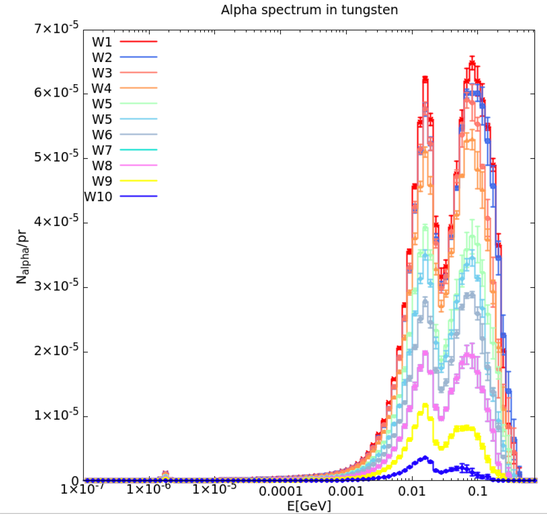

Science and Technology Facilities Council

ISIS Neutron and Muon Source

The FLUKA-CERN Updates on Neutronics

Recent important milestones in neutronics and significant progress achieved in neutronics simulations with FLUKA-CERN

- **Implementation of Point-Wise XS** and treatment (this allows explicit transportation of secondaries).
- **Enhanced Capabilities at low energy/temperature:** Improved simulation of low-energy neutrons, particularly thermal and cold neutrons, with available scattering kernels S(α,β,T) xs for numerous materials at low temperatures at various fixed temperatures.
- Expanded Data Library: **Users now have the flexibility to select from various data libraries** and file formats (e.g., ACE), enriching FLUKA's capabilities.
- Integration of Ncrystal in FLUKA (in progress): this is within a collaboration among ISIS, ESS and CERN
- Uploading meshed geometry from CAD files directly into FLUKA

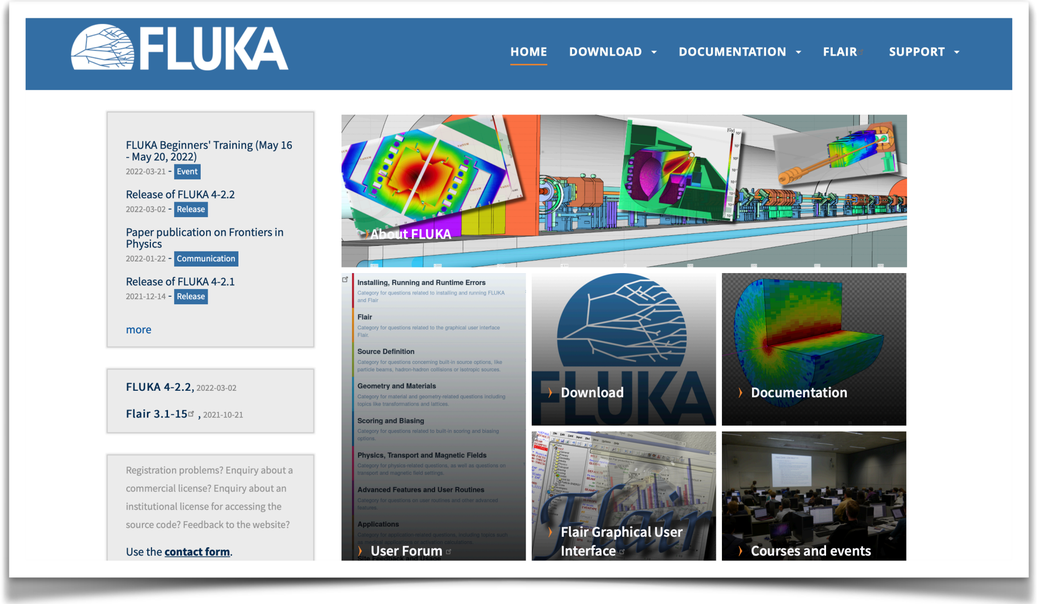

Important in the framework of future tasks in on development of “better designed” cold moderator for more efficient neutron source (ISIS-2, NEMESIS program):

https://web.infn.it/nemesis/

https://www.isis.stfc.ac.uk/about/future-of-isis/isis-ii/

DPA:
Definition and Implementation in FLUKA

Science and Technology Facilities Council
ISIS Neutron and Muon Source

DPA general Definition

Equivalent way to define DPA and way it is estimated in FLUKA

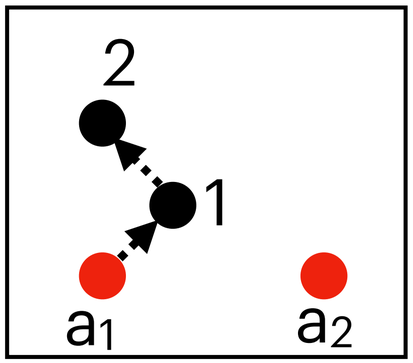

Represents the average number of times an atom in a material's crystal lattice is displaced from its original position due to irradiation:

atom1 is displaced twice,

atom2 is displaced 0,

on average an atom is displaced once

DPA =[times a_1 is displaced + times a_2 is displaced] / 2 Atoms

Represents the average number of displacements we count in a set of atoms from their original position due to irradiation.

2 displacements for atom1

0 displacement for atom2

On average the number of displacements are:

DPA = [2 displacements for a_1 + 0 displacements for a_2] / 2 Atoms

$$dpa \propto N_F$$

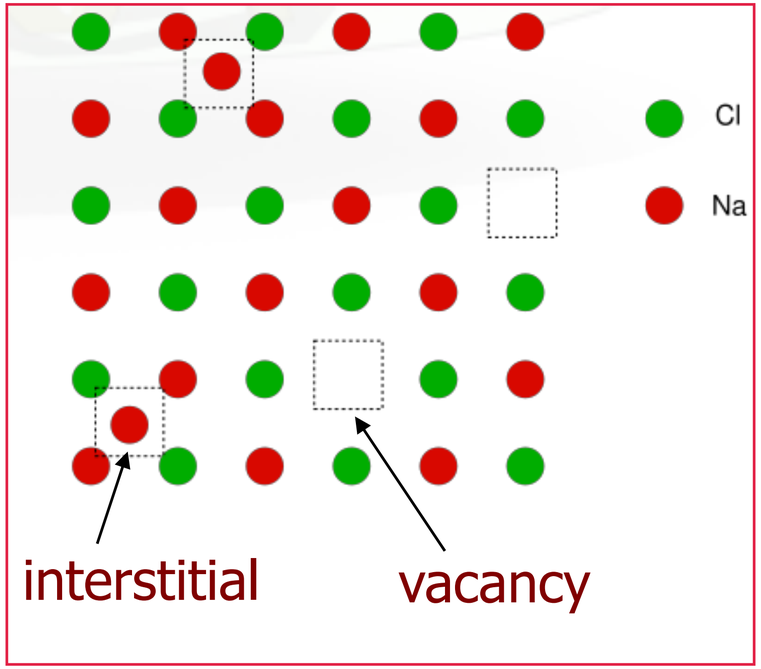

NF = number of defects (Frenkel pairs)

Each Frenkel pair originates from one displaced atom:

one vacancy (an atom missing from its lattice site), and

one interstitial (the same atom that has been displaced and now sits in a non-lattice position).

Multiple atoms dislodged create a cascade of Frenkel pairs

DPA-NRT vs ARC-dpa

Different efficiency transfer N (T_d)

DPA-NRT: Norgett Robinson Torrens model

$$N_{\mathrm{NRT}}(T_d) = \begin{cases} 0 & \text{if } 0 < T_d < E_d, \\ 1 & \text{if } E_d < T_d < \dfrac{2E_d}{0.8}, \\ \dfrac{0.8\,T_d}{2E_d} & \text{if } T_d > \dfrac{2E_d}{0.8}. \end{cases}$$

$$\mathrm{DPA}_x(E) = \frac{N_A \rho}{A_w} \int_{E_d}^{T_{\max}} dT \frac{d\sigma(E)}{dT} N_x(T_d),$$

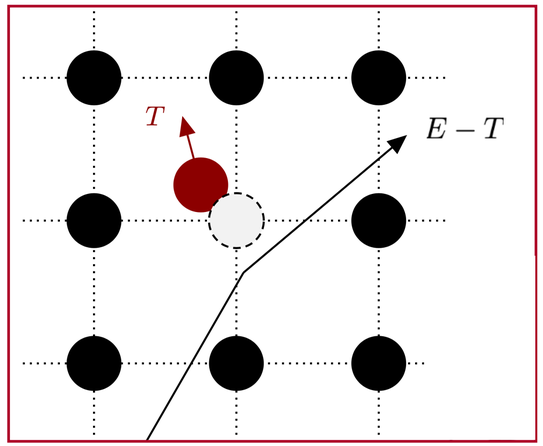

The binary collision simulations used as the basis of the NRT-DPA model focused, de facto, on the collisional phase of the displacement cascade and did not consider the dynamics of cascade evolution as atomic velocities fell down

Arc-dpa: Athermal Recombination Corrected DPA

$$N_{d,\text{arc-dpa}}(T_d) = \begin{cases} 0, & T_d < E_d, \\ 1, & E_d < T_d < 2E_d \\ \dfrac{0.8}{2E_d}\, T_d\, \xi_{\text{arc-dpa}}(T_d), & \dfrac{2E_d}{0.8} < T_d < \infty. \end{cases}$$

$$\xi_{\text{ARC-DPA}}(T_d) = \left(1 - c_{\text{arc-dpa}}\right)\left(\frac{2E_d}{0.8}\right)^{b_{\text{arc-dpa}}} T_d^{\,b_{\text{arc-dpa}}} + c_{\text{arc-dpa}}$$

It refines the more common NRT-dpa (Norgett-Robinson-Torrens) model by accounting for the recombination of Frenkel pairs (vacancies and interstitials) that occur during the displacement cascade (i.e recombination within overlapping cascades)

Material	E_d (eV)	$b_{\text{arc-dpa}}$	$c_{\text{arc-dpa}}$
Ni	39	-1.01 ± 0.11	0.23 ± 0.01
W&Ta	70	-0.56 ± 0.02	0.12 ± 0.01

Science and Technology Facilities Council

ISIS Neutron and Muon Source

DPA-NRT vs ARC-dpa

Different efficiency transfer N (T_d)

DPA-NRT: Norgett Robinson Torrens model

$$N_{\mathrm{NRT}}(T_d) = \begin{cases} 0 & \text{if } 0 < T_d < E_d, \\ 1 & \text{if } E_d < T_d < \dfrac{2E_d}{0.8}, \\ \dfrac{0.8\,T_d}{2E_d} & \text{if } T_d > \dfrac{2E_d}{0.8}. \end{cases}$$

The binary collision simulations usec the basis of the NRT-DPA mo focused, de facto, on the collisic phase of the displacement cascade did not consider the dynamics cascade evolution as atomic veloc fell down

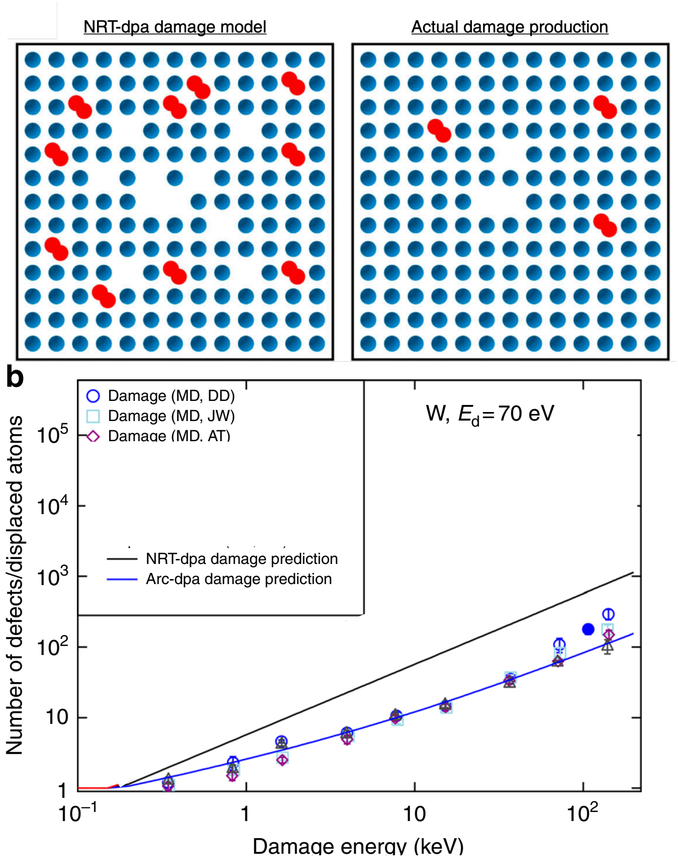

https://doi.org/10.1038/s41467-018-03415-5

Figure from Nature Communication,

Kai Nordlund et al,

Arc-dpa: Athermal Recombination Corrected DPA

$$N_{d,\text{arc-dpa}}(T_d) = \begin{cases} 0, & T_d < E_d, \\ 1, & E_d < T_d < 2E_d \\ \dfrac{0.8}{2E_d}\,T_d\,\xi_{\text{arc-dpa}}(T_d), & \dfrac{2E_d}{0.8} < T_d < \infty. \end{cases}$$

$$\xi_{\text{ARC-DPA}}(T_d) = \left(1 - c_{\text{arc-dpa}}\right)\left(\frac{2E_d}{0.8}\right)^{b_{\text{arc-dpa}}} T_d^{\,b_{\text{arc-dpa}}} + c_{\text{arc-dpa}}$$

It refines the more common NRT-dpa (Norgett-Robinson-Torrens) model by accounting for the recombination of Frenkel pairs (vacancies and interstitials) that occur during the displacement cascade (i.e recombination within overlapping cascades)

Material	E_d (eV)	$b_{\text{arc-dpa}}$	$c_{\text{arc-dpa}}$
Ni	39	-1.01 ± 0.11	0.23 ± 0.01
W&Ta	70	-0.56 ± 0.02	0.12 ± 0.01

Science and Technology Facilities Council

ISIS Neutron and Muon Source

FLUKA Model of ISIS-TS1 Target Reflector Moderator Assembly

Some technical details

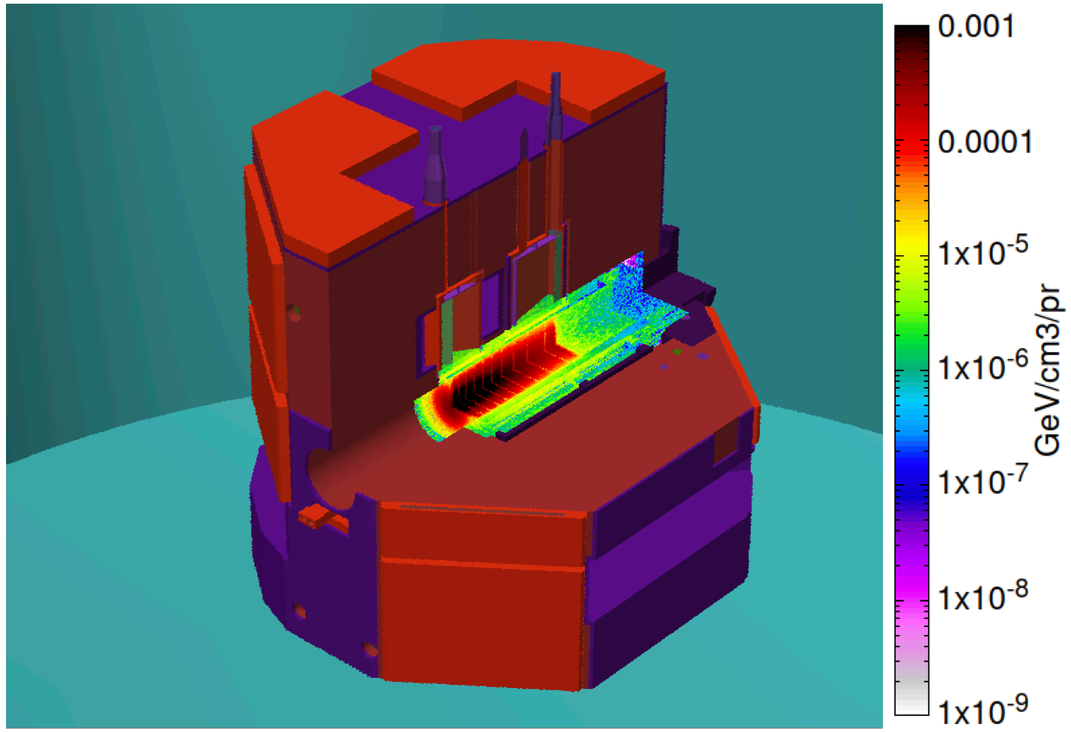

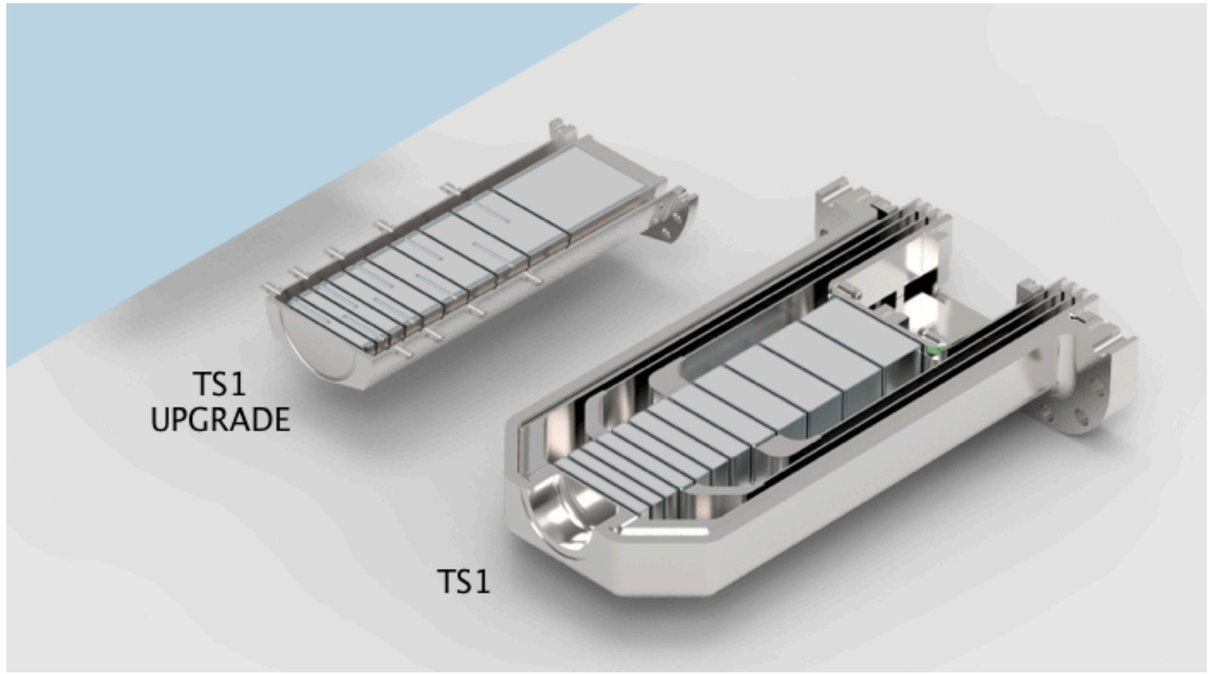

- Total mass TS1 target =61 kg (of which 46 kg is W)
- Segmented target(10 Plates) cooled by D2O
- Reflector reduced in size (edge cooled, multi brick Beryllium surrounded by Boral layer)

Plate *N*	t_W *[cm]*	W *V[cm³]*	Ta *V[cm³]*
1	1.1	82.341	40.522
2	1.2	89.884	41.804
3	1.4	104.970	44.367
4	1.6	120.056	46.931
5	1.6	120.056	46.931
6	1.9	142.685	50.776
7	2.3	172.857	55.903
8	2.9	218.115	63.594
9	3.7	278.458	73.848
10	14.3	1078.013	209.716

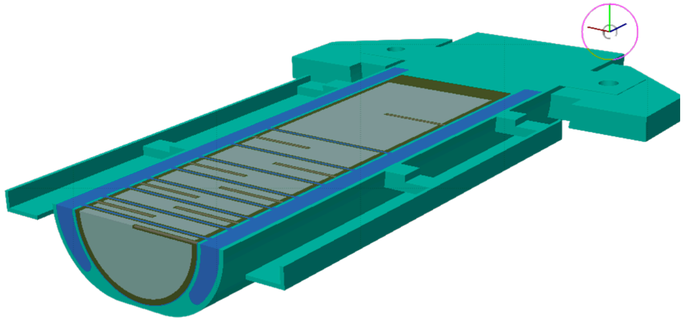

cooling channels between the plates are 2 mm wide. The target core is enclosed in a stainless-steel pressure vessel, and heavy water (D2O) coolant is pumped through the cooling channels

Science and Technology Facilities Council

ISIS Neutron and Muon Source

Upgraded Target TS1: FLUKA Simulation Results

Energy Deposition and particle fluence and fluence energy spectra

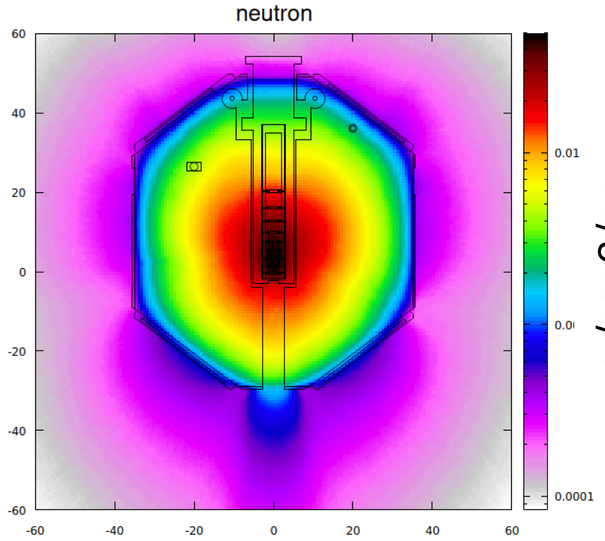

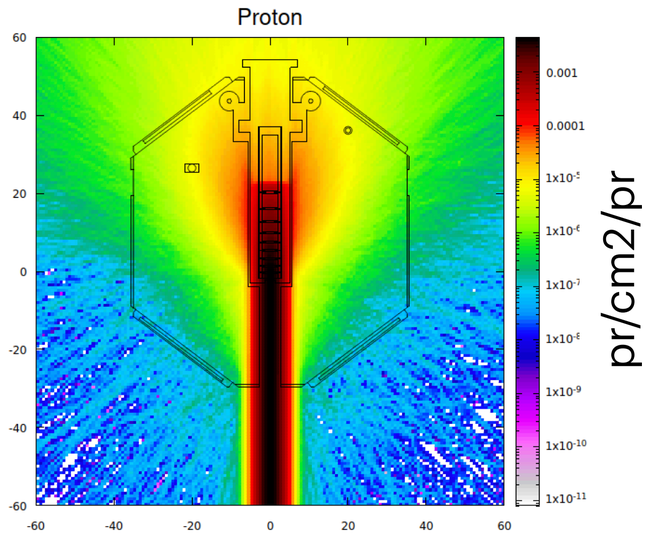

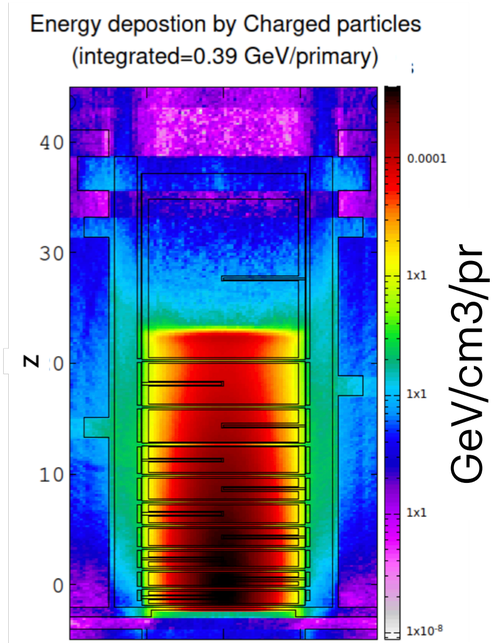

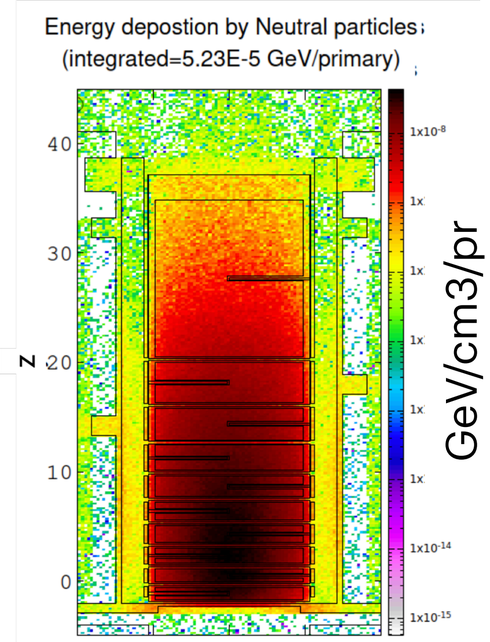

Table 3. Primary beam characteristics.

Proton Beam			
Energy profile		**Spatial profile**	
Distrib.	Gaussian	Distrib.	Gaussian
Mean E	800 MeV	FWHM	4.215 cm
ΔE	±0.4%	Div. H/Div. V	100-90 π mm·mrad
FWHM	7.4 MeV	Ang. div.	0.88 mrad

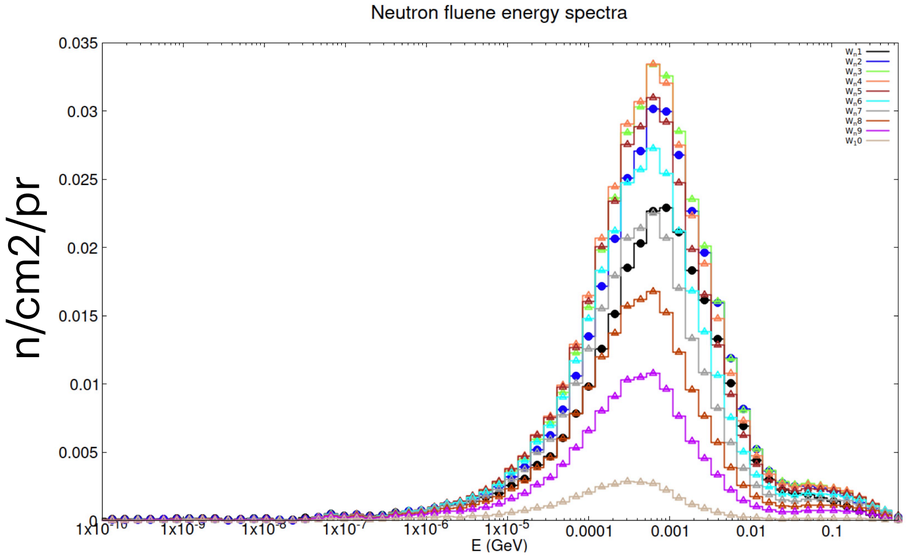

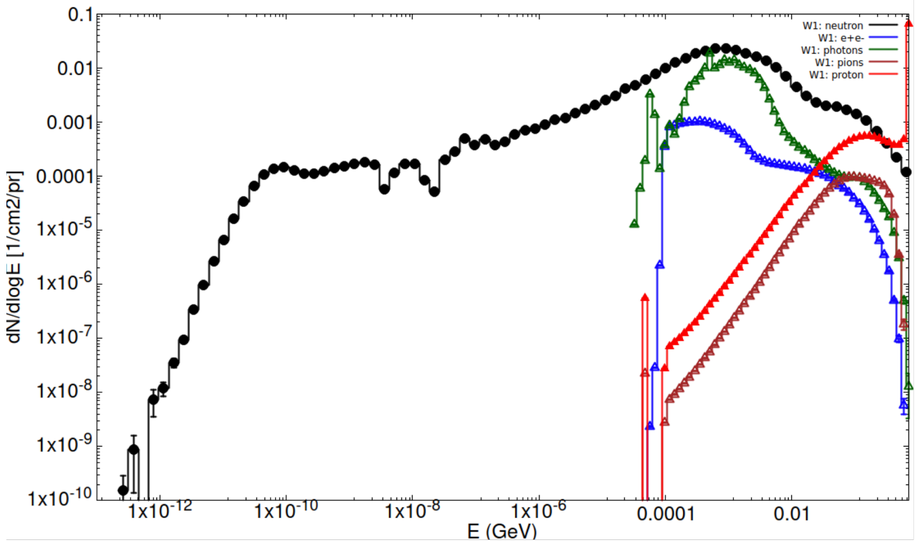

Science and Technology Facilities Council

ISIS Neutron and Muon Source

Benchmarking FLUKA Models of TS1 TRAM

a

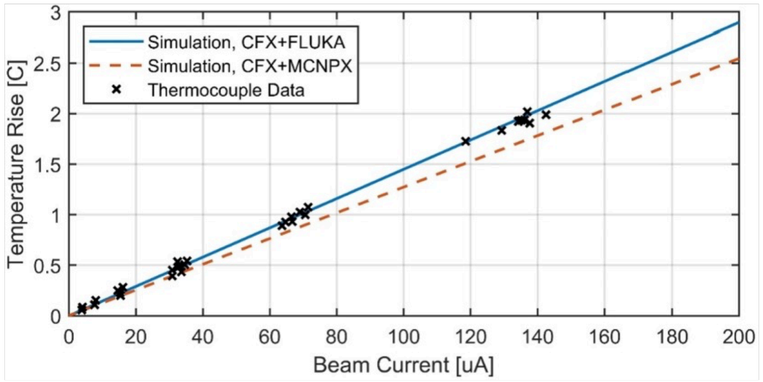

b

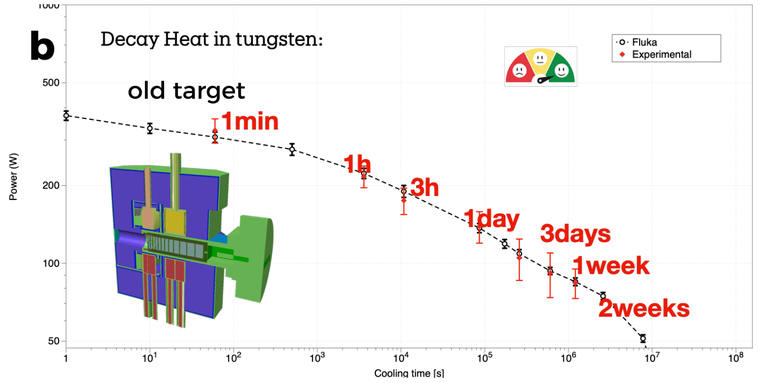

c

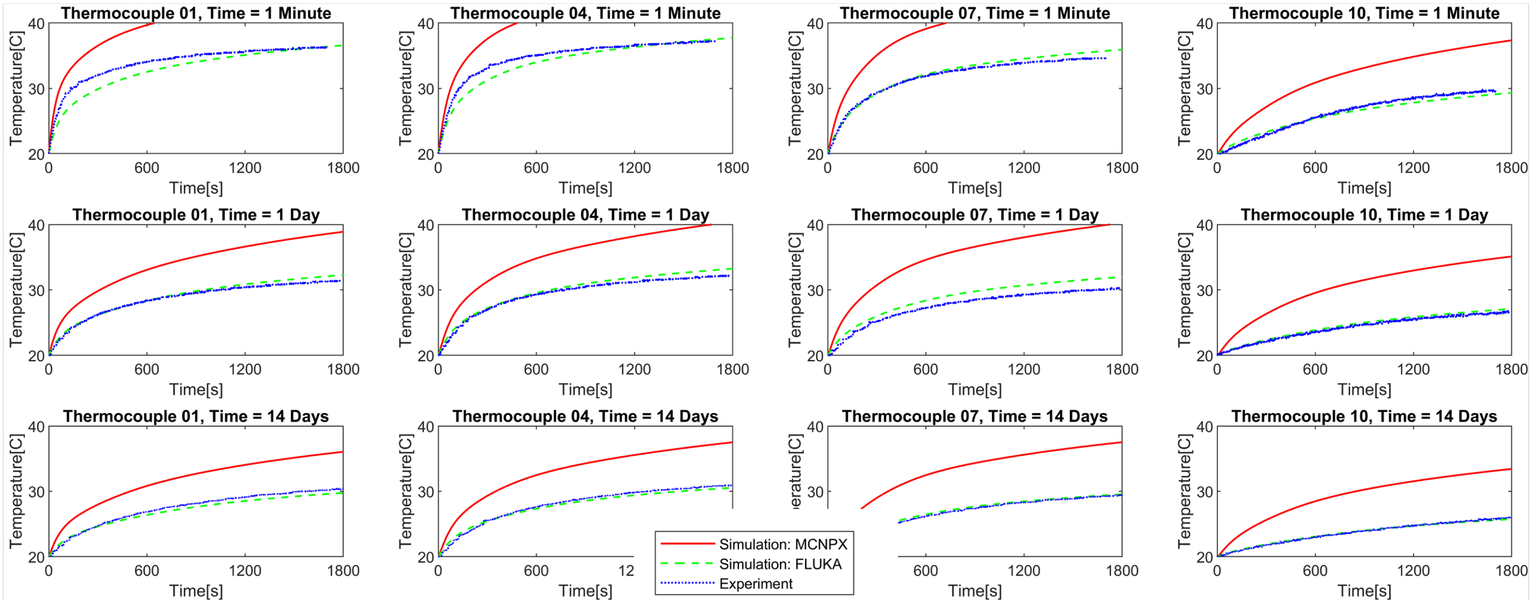

Science and Technology Facilities Council

ISIS Neutron and Muon Source

- The FLUKA models of the TS1 targets (new and old) have been successfully validated wrt Power depostion, Decay Heat, RN inventory

Published works

D. Wilcox et al., "Simulated and measured performance of the ISIS TS-1 Project target", Journal of Neutron Research, vol. 26, pp. 47–58, 2024.

Journal of Neutron Research 24 (2022) 313–327
DOI 10.3233/JNR-220030
IOS Press

Decay heat in ISIS spallation target: simulations and measurements

Lina Quintieri *, Steven Lilley, Dan Wilcox, David Findlay, David Jenkins, Stephen Gallimore and David Haynes
ISIS Neutron and Muon Source, Rutherford Appleton Laboratory STFC, OX11 0QX, Didcot, United Kingdom

Radionuclei inventory in ISIS TS1 target: measurements and comparison with FLUKA-CERN predictions

Lina Quintieri[1,*], *Steven* Lilley[1], *Dan* Wilcox[1], *Xavier* Ortego[2], *Gordon* Burns[1], and *Angelo* Grossi[2]
[1]ISIS Neutron and Muon Source, Rutherford Appleton Laboratory STFC, OX11 0QX, Didcot, United Kingdom
[2]ENEA, Dept. of Fusion and Technologies for Nuclear Safety and Security, Centro Ricerche Casaccia, Anguillara (Roma), Italy

In press on EPJ Web Of Conferences

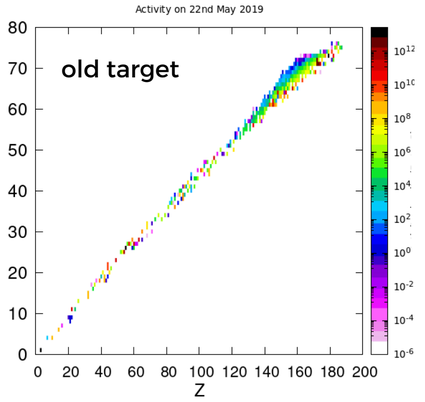

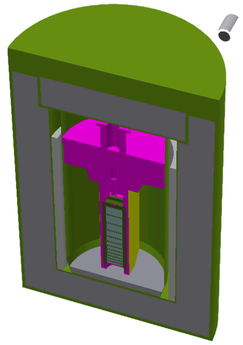

. Estimated overall RN activity in the target on

DPA in TS1 Target

usrbin:spatial mesh for Avg and peak values in whole target

(W+Ta) target	DPA-SCO	DPA-NRT	ARC-DPA
Monte Carlo Rate [dpa/primary]			
AVG*	$7.5 \times 10^{-23} \pm 5\%$	$2.5 \times 10^{-22} \pm 4\%$	$6.7 \times 10^{-23} \pm 4\%$
PEAK	$2.1 \times 10^{-22} \pm 15\%$	$5.8 \times 10^{-22} \pm 15\%$	$1.4 \times 10^{-22} \pm 15\%$
Dpa rate [dpa s^{-1}] (200 μA proton beam)			
AVG*	9.4×10^{-8}	3.1×10^{-7}	8.4×10^{-8}
PEAK	2.6×10^{-7}	7.2×10^{-7}	1.75×10^{-7}
Estimated dpa in one year [dpa][a]			
AVG*	3	10	2.6
PEAK	8	22	5.5
Dose per Amp-hour [dpa/Ah]			
AVG*	1.69	5.58	1.51
PEAK	4.68	12.96	3.15

[a] Values estimated under the assumption of continuous operation at full beam current (24 h/day, 365 days/year).

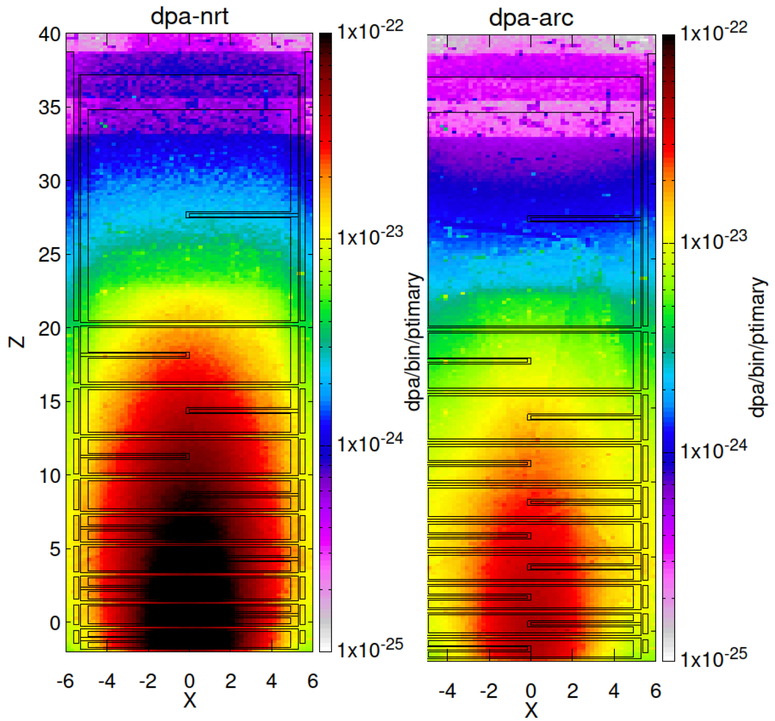

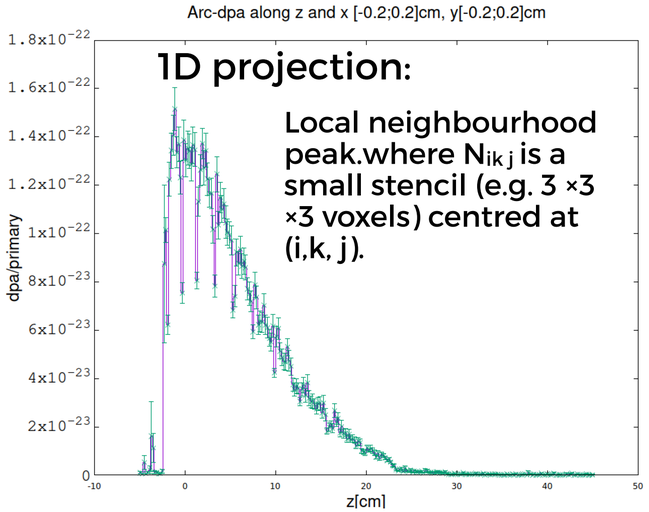

Ed

- Tungsten 70 ev
- Tantalum 70 eV
- Iron 40 eV
- Nickel 40 eV

THE DPA-NRT approach provides radiation damage value significantly higher (a factor 4 approx) than the ARC-dpa, especially in the high-intensity region near the beam impact point.

ARC-DPA reflect their more realistic treatment of damage production (incorporating the recombination of point defects during the displacement cascade, which reduces the effective number of surviving Frenkel pairs)

The spatial patterns are broadly consistent across the 2 models, with a maximum in the first plates where the proton interactions are most intense, and a gradual decrease along the target depth.

* The avg values here reported corresponds to the maximum among all the mean values for each region (i.e plate)

Distinguishing contributions: neutral vs charged particles

neutral part.

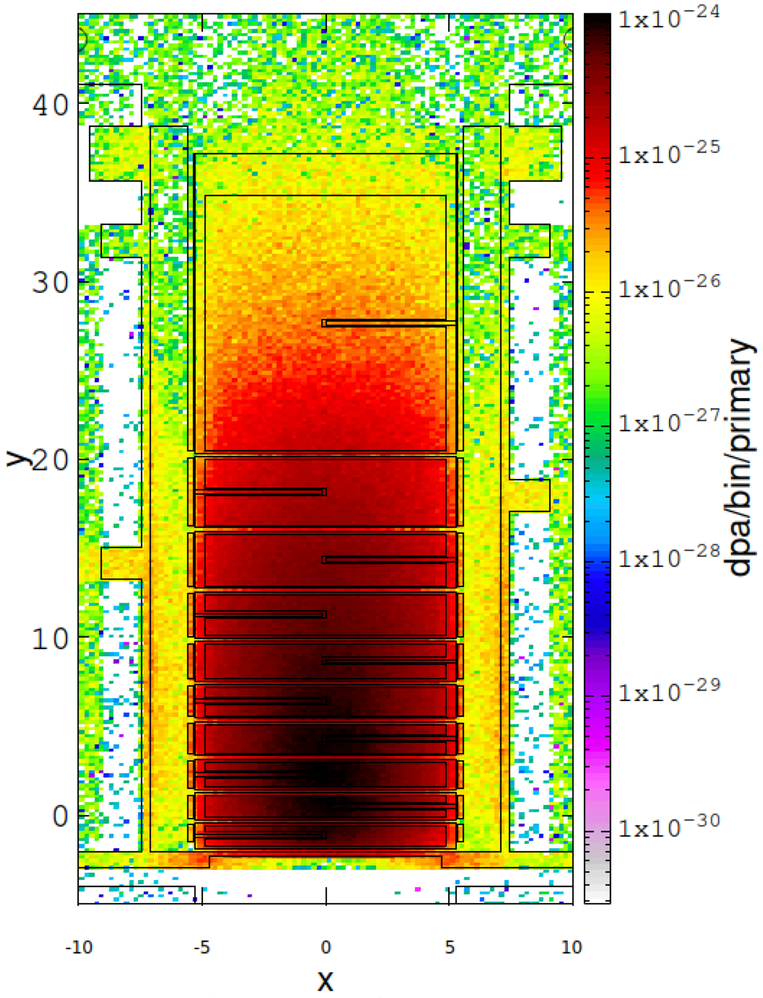

mostly isotropic

charged part.

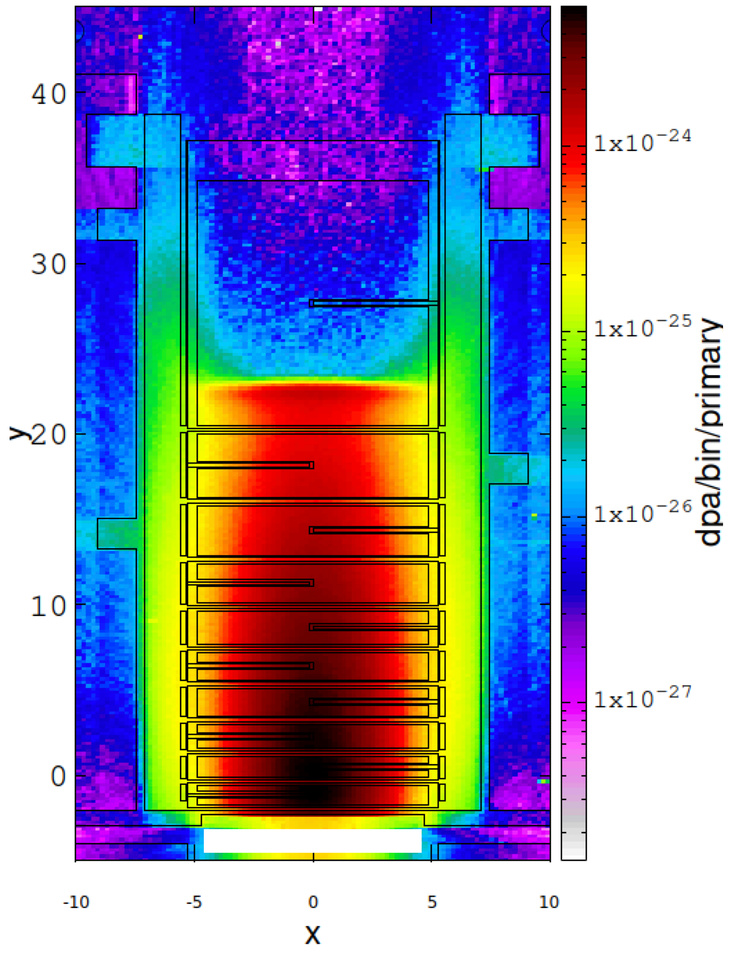

mainly proton beam footprint

Figure shows the ARC-DPA contributions from charged particles (right) and neutral (left).

It is evident that the dominant contribution to displacement damage originates from charged hadrons, primarily protons, which produce the highest DPA levels concentrated in the region where the beam penetrates the target.

In contrast, the DPA induced by neutrons follows a different spatial pattern, characterised by a more diffuse and extended distribution across the target plates. This highlights the distinct roles of neutral and charged particles in the overall radiation damage process.

Plate by Plate Results

usrbin region: avg DPA in region

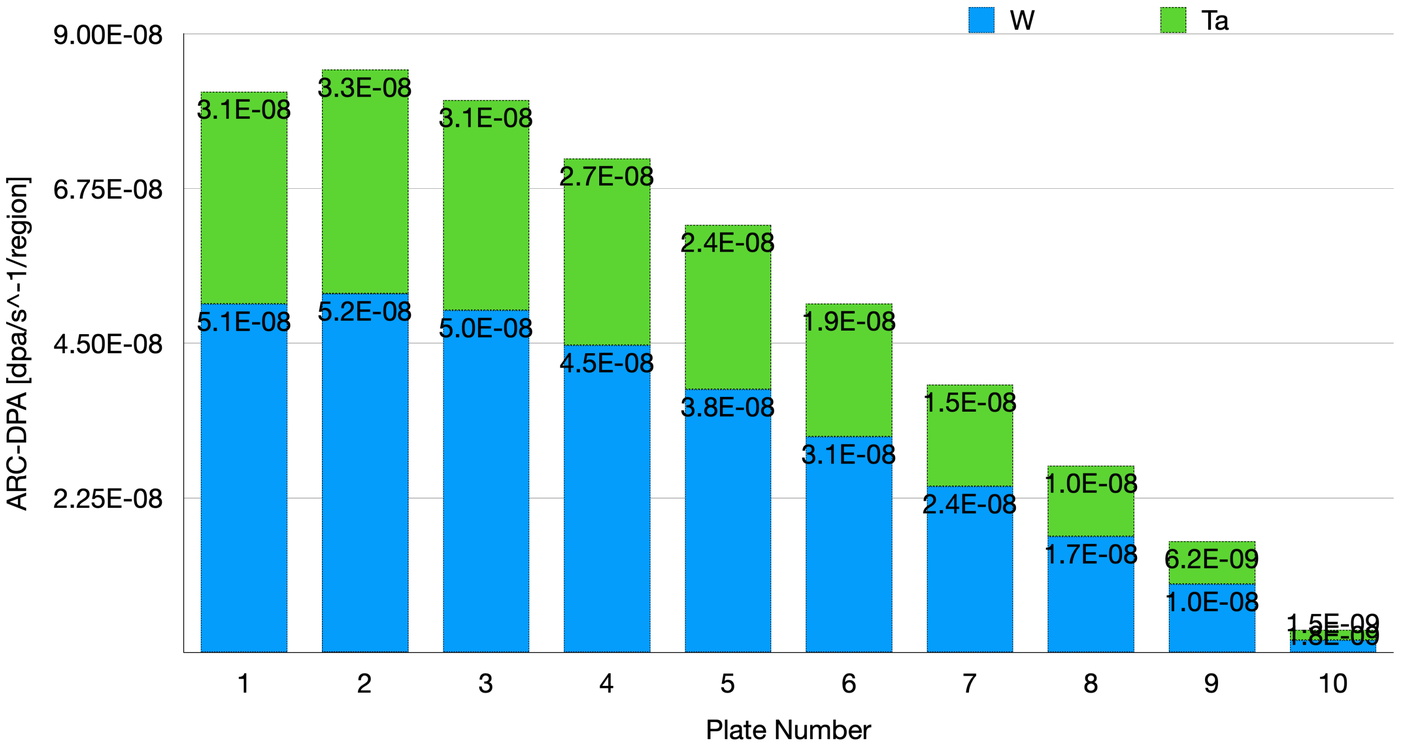

ARTICLE NATURE COMMUNICATIONS | DOI: 10.1038/s41467-018-03415-5

Table 1 Material constants

Material	E_d (eV)	$b_{arc\text{-}dpa}$	$c_{arc\text{-}dpa}$	$b_{rpa\ (eV)}$	c_{rpa}
Fe	40	−0.568 ± 0.020	0.286 ± 0.005	1018 ± 145	0.95 ± 0.04
Cu	33	−0.68 ± 0.05	0.16 ± 0.01	3319 ± 249	0.97 ± 0.02
Ni	39	−1.01 ± 0.11	0.23 ± 0.01	3325 ± 230	0.92 ± 0.01
Pd	41	−0.88 ± 0.12	0.15 ± 0.02	2065 ± 183	1.08 ± 0.02
Pt	42	−1.12 ± 0.09	0.11 ± 0.01	5531 ± 762	0.87 ± 0.02
W	70	−0.56 ± 0.02	0.12 ± 0.01	12,332 ± 1250	0.73 ± 0.01

Results for the arc-dpa and rpa material constants for a number of metals. The errors are given in s.e.m.

```
MAT-PROP    Type: DPA-ENER ▾ DPA Eth: 70.
            b_arcdpa: -0.56   c_arcdpa: 0.12
            Mat: TUNGSTEN ▾ to Mat: ▾        Step:
MAT-PROP    Type: DPA-ENER ▾ DPA Eth: 70.
            b_arcdpa: -0.56   c_arcdpa: 0.12
            Mat: TANTALUM ▾ to Mat: ▾        Step:
MAT-PROP    Type: DPA-ENER ▾ DPA Eth: 40
            b_arcdpa: -0.568  c_arcdpa: 0.286
            Mat: Stainles ▾   to Mat: ▾      Step:
MAT-PROP    Type: DPA-ENER ▾ DPA Eth: 40.
            b_arcdpa: -0.568  c_arcdpa: 0.286
            Mat: IRON ▾       to Mat: ▾      Step:
MAT-PROP    Type: DPA-ENER ▾ DPA Eth: 20.
            b_arcdpa:         c_arcdpa:
            Mat: CARBON ▾     to Mat: ▾      Step:
MAT-PROP    Type: DPA-ENER ▾ DPA Eth: 39.
            b_arcdpa: -1.01   c_arcdpa: 0.23
            Mat: NICKEL ▾     to Mat: ▾      Step:
```

Very conservative assumption: continuous operation at 200 μA (365 days a year), the most exposed plates (P2) should get:

W:

- **1.64 dpa –> 1 year** (already enough to produce a strong drop in room-temperature thermal conductivity in pure W);
- **4.9 dpa –> 3 years** (serious long-term structural/property degradation territory, depending strongly on irradiation temperature and material grade)

Ta

- **1.04 dpa –> 1 year**
- **3.12 dpa –> 3 years**

NB. TFrom litterature we know that antalum performs better with respect to radiation damaging, alloying tungsten with tantalum (W-Ta) has been shown to improve radiation tolerance by suppressing d-fect generation and enhancing recombination processes, resulting in less degradation of thermal properties com-pared to pure W, although the intrinsic thermal conductivity of W-Ta alloys remains lower than that of pure tungsten

$$\text{appm} = \frac{10^6 \, N_{\text{imp}}}{\left(\frac{m}{A}\right) N_A},$$

Plate by Plate Results

usrbin region and/or RESNUCLEI: helium production

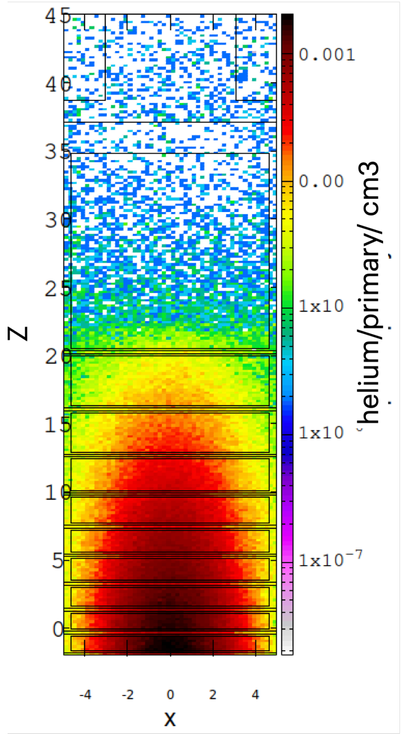

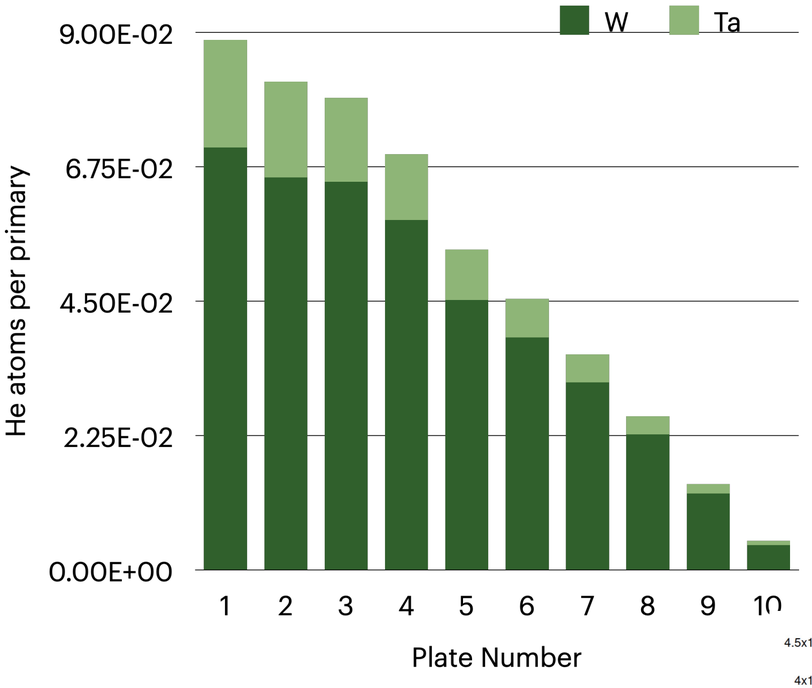

($I_p = 200\mu A$)

He concentration in W and Ta plates.

^{4}He in ISIS TS1 plates		
Plate	W [appm/s^{-}]	Ta [appm/s^{-}]
P1	$1.687\ 10^{-5}$	$1.047\ 10^{-5}$
P2	$1.437\ 10^{-5}$	$9.159\ 10^{-6}$
P3	$1.218\ 10^{-5}$	$7.772\ 10^{-6}$
P4	$9.612\ 10^{-6}$	$5.927\ 10^{-6}$
P5	$7.414\ 10^{-6}$	$4.526\ 10^{-6}$
P6	$5.373\ 10^{-6}$	$3.354\ 10^{-6}$
P7	$3.583\ 10^{-6}$	$2.296\ 10^{-6}$
P8	$2.054\ 10^{-6}$	$1.357\ 10^{-6}$
P9	$9.079\ 10^{-7}$	$6.587\ 10^{-7}$
P10	$7.671\ 10^{-8}$	$1.334\ 10^{-7}$

He concentration in W and Ta plates.

^{4}He in ISIS TS1 plates		
Plate	W [appm/Ah]	Ta [appm/Ah]
P1	303.66	188.46
P2	258.66	164.862
P3	219.24	139.896
P4	173.016	106.686
P5	133.452	81.468
P6	96.714	60.372
P7	64.494	41.328
P8	36.972	24.426
P9	16.3422	11.8566
P10	1.38078	2.4012

Under the hypothetical scenario of continuous irradiation with a 200 μA proton current,

on average, a concentration **of 1 appm is reached after about 23 hours** of irradiation in plates P1 to P3.

With prolonged exposure, the threshold of 10 appm is attained after roughly 10 days, while concentrations **exceeding 100 appm** are reached after a slightly longer period three months in plate P1-P3

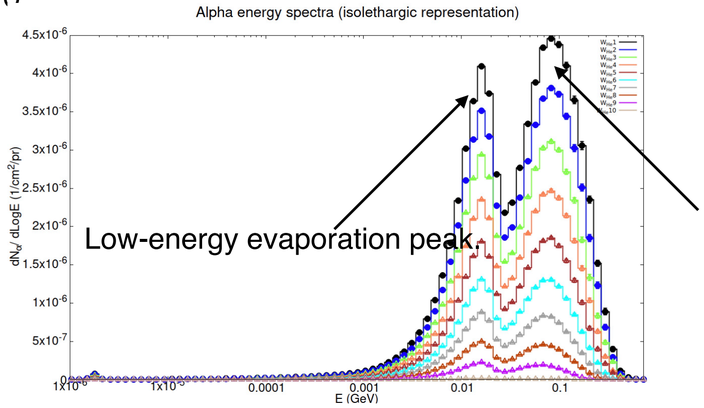

Figure 22. ^4He energy spectrum estimated within the W core of each target plate (USRTRACK results normalised by volume)

fast nucleons near the nuclear surface can coalesce into light clusters (d, t, 3He, ς) and escape before the system reaches equilibrium.

$$\text{appm} = \frac{10^6 \, N_{\text{imp}}}{\left(\frac{m}{A}\right) N_A},$$

Plate by Plate Results

usrbin region and/or RESNUCLEI: H isotope production

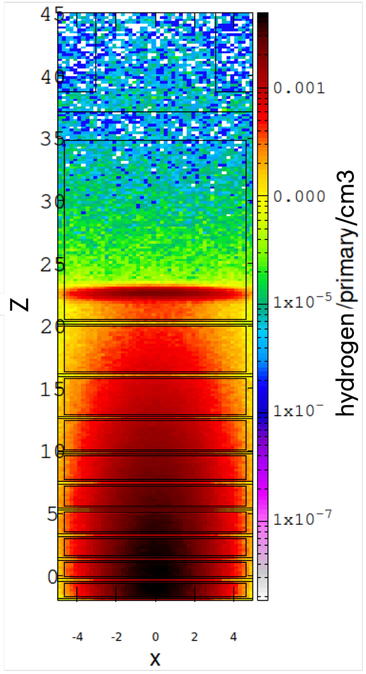

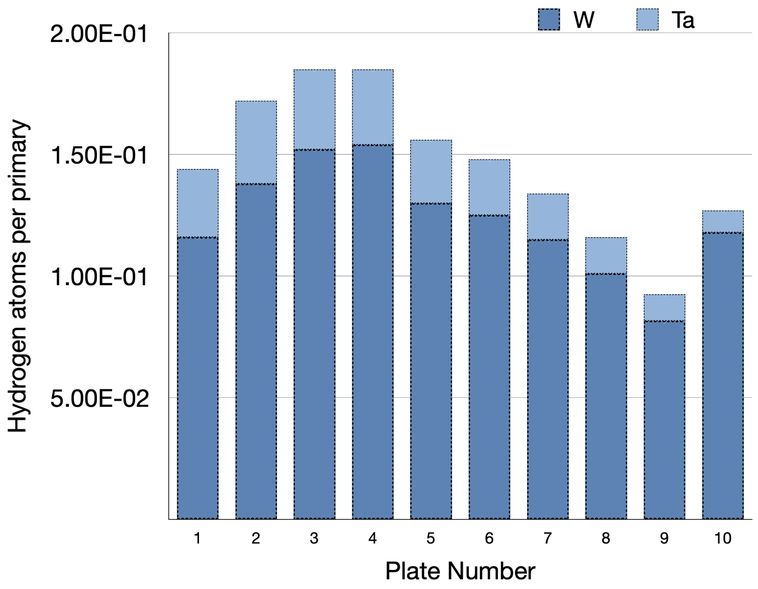

Hydrogen concentration plate by plate ($I_p = 200\mu$

^{1}H in ISIS TS1 plates		
Plate	W [appm/s]	Ta [appm/]
P1	2.768E-05	1.628E-05
P2	3.018E-05	1.946E-05
P3	2.849E-05	1.832E-05
P4	2.526E-05	1.670E-05
P5	2.132E-05	1.401E-05
P6	1.727E-05	1.187E-05
P7	1.312E-05	9.282E-06
P8	9.140E-06	6.785E-06
P9	5.788E-06	4.529E-06
P10	2.166E-06	1.691E-06

Hydrogen concentration plate by plate

^{1}H in ISIS TS1 plates		
Plate	W [appm/Ah]	Ta [appm/Ah
P1	498.24	293.04
P2	543.24	350.28
P3	512.82	329.76
P4	454.68	300.6
P5	383.76	252.18
P6	310.86	213.66
P7	236.16	167.076
P8	164.52	122.13
P9	104.184	81.522
P10	38.988	30.438

Hydrogen production in the whole target is both higher in absolute yield (of a factor almost 2.5) and more broadly distributed within the target, owing to its multiple reaction pathways, including spallation, fragmentation, and secondary processes that extend over the full target geometry.

Under the hypothetical scenario of continuous irradiation with a 200 μA proton current, on average, a concentration **of 1 appm is reached after about 20 hours** of irradiation in most of the plates (P1 to P7).

With prolonged exposure, the threshold of 10 appm is attained after roughly 10 days, while concentrations **exceeding 100 appm** are reached after about three months in the majority of the plates.

Benchmarking DPA Predictions

Science and Technology Facilities Council
ISIS Neutron and Muon Source

Direct and Indirect Approaches to Measuring Thermal Conductivity

Direct Method

- Steady-State: $k = \frac{QL}{A\Delta T}$
- Measures heat flow and ΔT

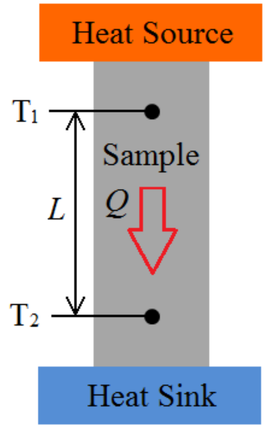

https://www.linseis.com/en/instruments/thermal-conductivity/lfa-l52/

Indirect method

- Laser Flash: $\alpha = \frac{k}{\rho c_p}$
- Measures T—> α → k derived

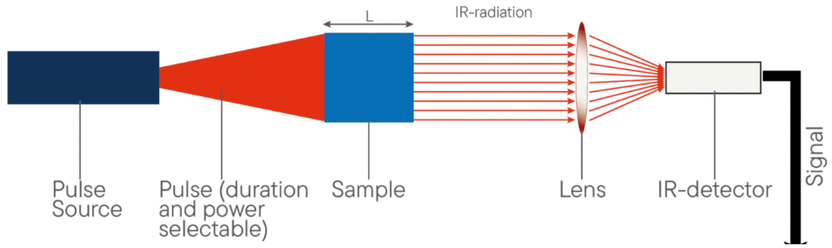

https://arxiv.org/pdf/1605.08469

Inverse estimation of k- Model based

In operando method as proposed by D. Findlay. Fitting the plate temperature profile, read with thermocouple, during cooling phase

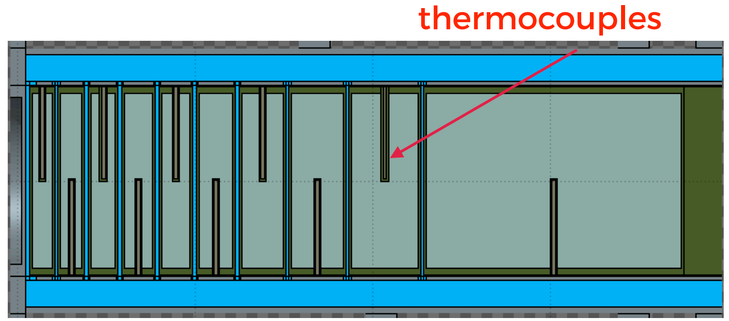

In Fluka TS1-target model thermocouple are implemented

"Results have been obtained from direct measurements ***on an operating spallation target****,"*

https://doi.org/10.1016/j.nima.2026.171555

Science and Technology Facilities Council

ISIS Neutron and Muon Source

Measurement Campaign at ISIS: 2 Irradition Scenarios

Decrease of thermal conductivity: is caused primarily by introducing defects like point defects and dislocation loops into the material's lattice structure, which scatter phonons and electrons, thereby decreasing their mean free path and increasing thermal resistance.

Scenario	G_{D2O} [L/min]	I [μA]	T_{p2} [C]	T_{p9} [C]
6 mAh	476	134	150	86
935 mAh	485	147	150	86

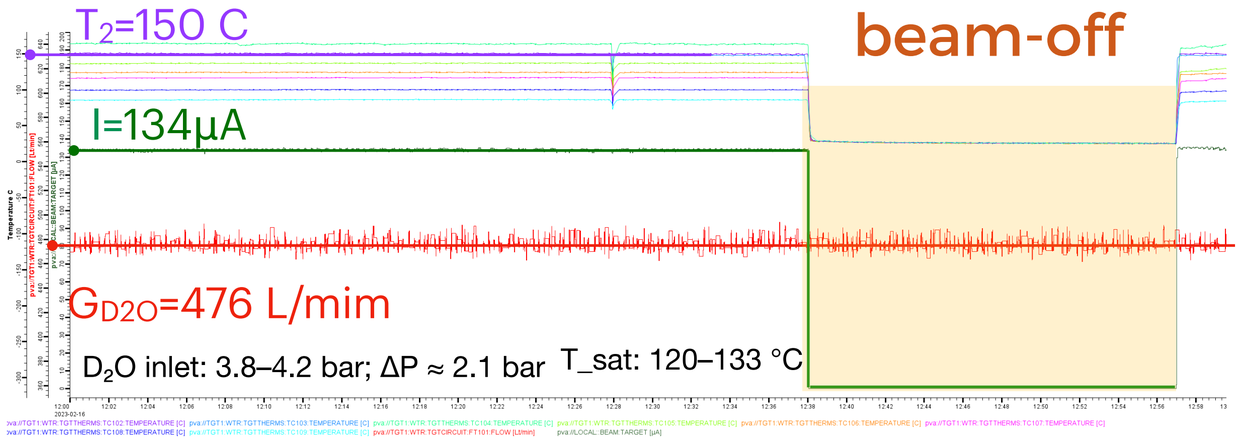

Scenario1 - test on 16-02-2023

·https://doi.org/10.1016/j.nima.2026.171555. "Measurements of decreasing tungsten thermal conductivity in an operating spallation neutron target"

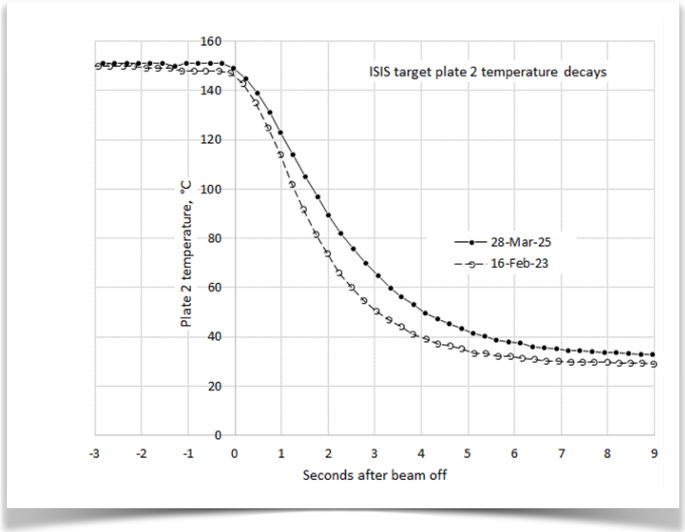

$$\alpha = k/(\rho c)$$

$$\tau_{cond} \sim \frac{L^2}{\alpha},$$

A reduction in effective thermal conductivity means slowing down the redistribution of heat from the plate core toward the cooled surfaces.

As a consequence, even if the external convective coefficient remains comparable, the central temperature exhibits a smaller initial slope and a slower cooldown.

Thermal Conductivity in Tungsten as a Function of cDPA

D. R. Mason, A. Reza, F. Granberg, and F. Hofmann, "An estimate for thermal diffusivity in highly irradiated tungsten using molecular dynamics simulation," Phys-cal Review Materials, vol. 5, p. 125407, 2021

Model based on MD simualtions

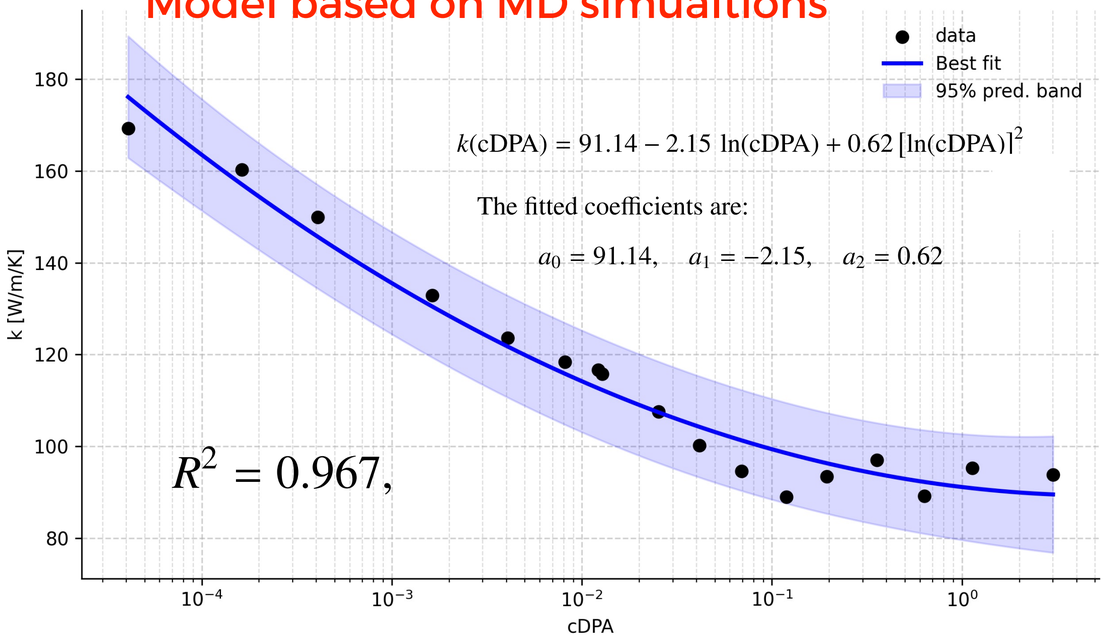

Model for computing the thermal diffusivity of tungsten, based on the conductivity of the perfect crystal and resistivity per Frenkel pair, and dividing a simulation into perfect and athermal regions statistically.

Plate	cDPA (6 mA·h)	k (6 mA·h) [W/mK]	cDPA (935 mA·h)	k (935 mA·h) [W/mK]
P1	5.47E-3	119.1	0.853	91.5
P2	5.63E-3	118.9	0.88	91.4
P3	5.37E-3	119.3	0.84	91.5
P4	4.82E-3	120.3	0.75	91.8
P5	4.13E-3	121.6	0.64	92.2
P6	3.38E-3	123.4	0.53	92.8
P7	2.61E-3	125.9	0.41	93.6
P8	1.82E-3	129.4	0.283	94.8
P9	1.07E-3	134.9	0.17	96.9
P10	1.93E-4	154.9	0.0304	106.2

The uncertainty on the thermal conductivity was obtained by propagating the uncertainty on cDPA through Eq. *, using a first-order (linear) error propagation approach and combining quadratically with the uncertainty of the fit: $U_{k,\mathrm{tot}} = \sqrt{U_{k,\mathrm{fit}}^2 + U_{k,\mathrm{dpa}}^2}$.

Scenario	Plate	cDPA dose	e(cDPA)	k [W/cmK]	e_k* [W/cmK]
6 mA·h	P2	5.63×10^{-3}	$\pm 1.22 \times 10^{-3}$	1.19	± 0.12
935 mA·h	P2	0.88	± 0.17	0.91	± 0.08

Sensitivity to: Proton beam current variations (5%), Beam spot size variations (10% variation of the FWHM of the Gaussian spatial distribution), Nuclear data uncertainty, effective mA·h for the irradiation scenario (10%),

FLUKA Predictions for Scenario1 and Scenario2

Comparison with experimental results from method based on D.Findlay et al work

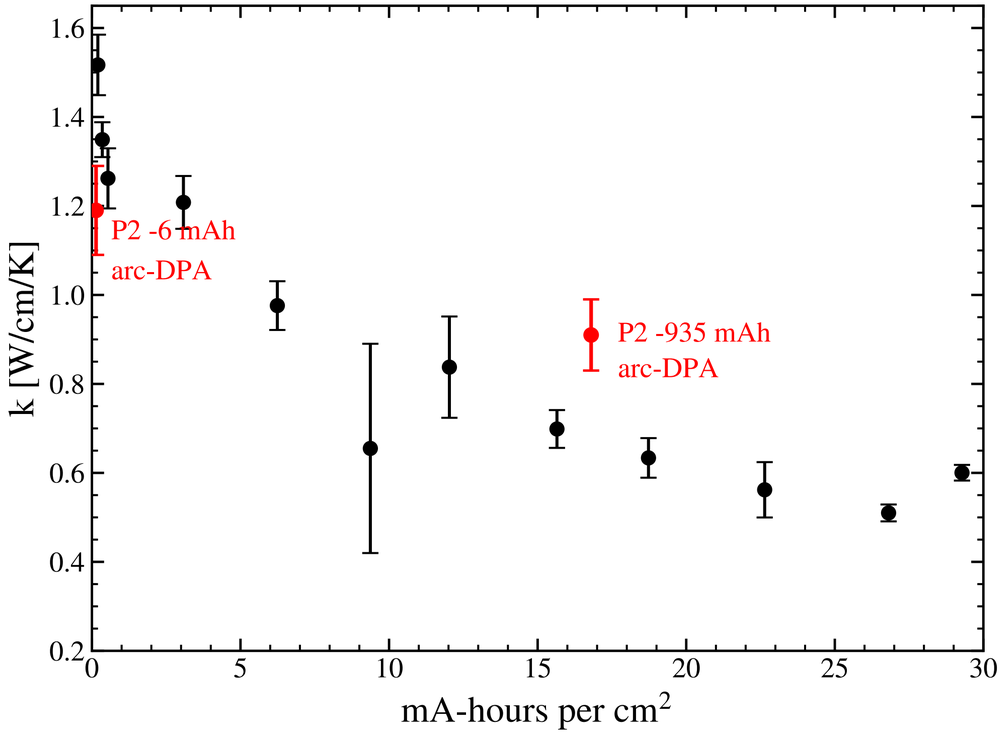

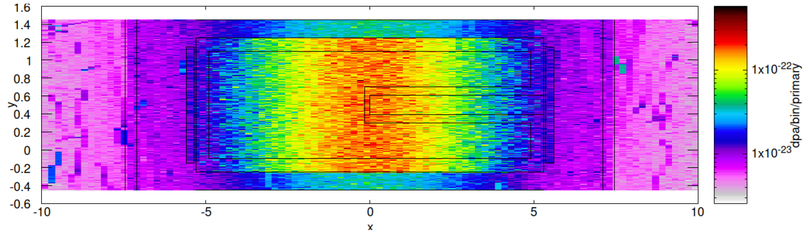

Spatial distribution of ARC-DPA in Plate2

The thermal conductivity values derived from FLUKA predictions, using Model of Mason et al, are overall consistent with the experimental measurements, with good agreement within the associated uncertainties.

The main discrepancy is observed for plate 2 at highly irradiated scenario (935 mA· h) case, where the calculations based on FLUKA predict a smaller degradation of thermal conductivity driven by the DPA contribution, **with a difference of less than 20%** between the experimentally inferred from temperature profile fitting (D. Findlay et al) in and calculated values of k.

Final Benchmarking k(DPA-NRT) for Tungsten

In Findlay work: 1 DPA has been estimated equivalent to 5.38 mAh cm^{-2}

Habaniya values measured at PSI with LFA

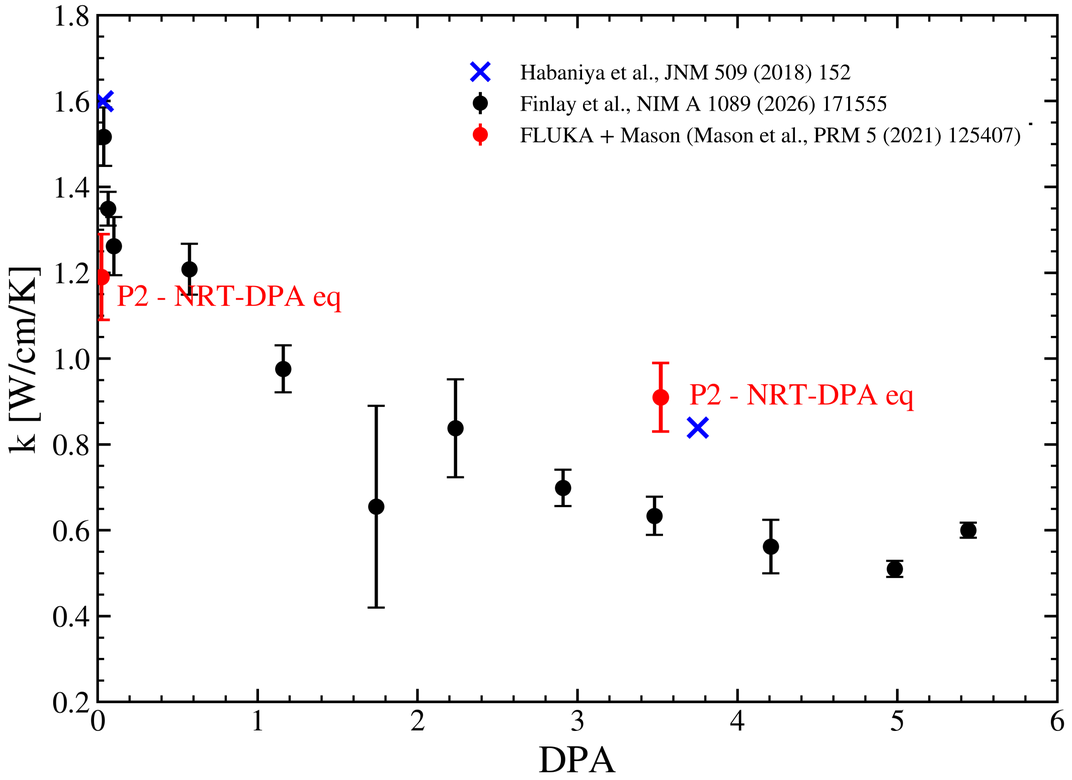

These preliminary results show that the k(cdpa) value of irradiated W derived by using FLUKA predictions are in quite good agreement with experimental data, **showing a better agreement with D.Findaly method at low irradiation and a closer match with Habaniya for higher irradiation**

- The Mason K(cDPA) provides a model to link thermal conductivity with Arc-DPA
- FLUKA predictions on the plot have been located according the correspondence between DPA-NRT and ARC-DPA as reported in the table below (ARC-DPA almost a factor 4 lower than DPA-NBRT)

FLUKA

Plate	dpa-arc dose [−]	dpa-nrt dose [−]
W1	5.47×10^{-3}	2.18×10^{-2}
Ta1	3.33×10^{-3}	1.30×10^{-2}
W2	5.63×10^{-3}	2.17×10^{-2}
Ta2	3.51×10^{-3}	1.32×10^{-2}
W3	5.37×10^{-3}	2.02×10^{-2}
Ta3	3.30×10^{-3}	1.20×10^{-2}
W4	4.82×10^{-3}	1.78×10^{-2}
Ta4	2.93×10^{-3}	1.05×10^{-2}
W5	4.13×10^{-3}	1.50×10^{-2}
Ta5	2.58×10^{-3}	0.91×10^{-2}
W6	3.38×10^{-3}	1.21×10^{-2}
Ta6	2.09×10^{-3}	0.72×10^{-2}
W7	2.61×10^{-3}	0.92×10^{-2}
Ta7	1.60×10^{-3}	0.54×10^{-2}
W8	1.82×10^{-3}	0.62×10^{-2}
Ta8	1.12×10^{-3}	0.37×10^{-2}
W9	1.07×10^{-3}	0.35×10^{-2}
Ta9	6.69×10^{-4}	0.21×10^{-2}
W10	1.93×10^{-4}	0.06×10^{-2}
Ta10	1.64×10^{-4}	0.05×10^{-2}

Plate	dpa-arc dose [−]	dpa-nrt dose [−]
W1	0.853	3.4
Ta1	0.52	2.03
W2	0.88	3.39
Ta2	0.55	2.06
W3	0.84	3.15
Ta3	0.514	1.87
W4	0.75	2.77
Ta4	0.46	1.63
W5	0.64	2.34
Ta5	0.41	1.41
W6	0.53	1.88
Ta6	0.33	1.12
W7	0.41	1.43
Ta7	0.25	0.84
W8	0.283	0.97
Ta8	0.174	0.57
W9	0.17	0.55
Ta9	0.10	0.33
W10	0.0304	0.09
Ta10	0.025	0.08

Can We Reproduce the Experimental T Profile with k "Degraded" Values ?

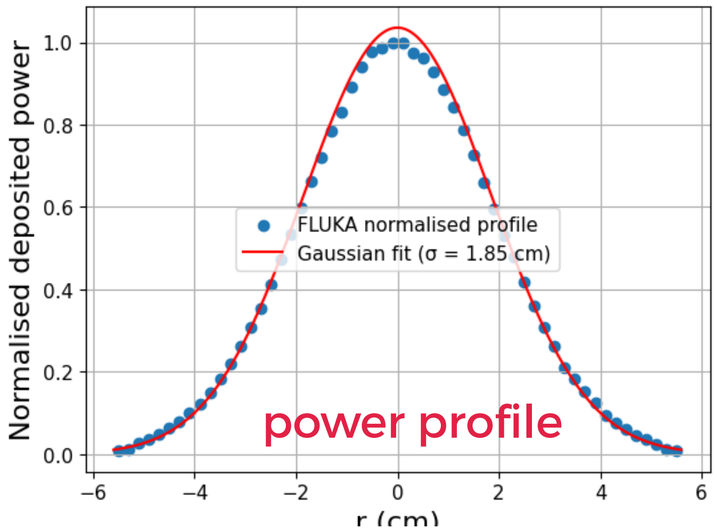

ANSYS

h(T)

$$h_1(T) = 2000\text{-}2500\ \text{W m}^{-2}\text{K}^{-1}, \quad \text{for } T = 303\text{-}373\ \text{K}$$
$$h_2(T) = 2500\text{-}30000\ \text{W m}^{-2}\text{K}^{-1}$$

Parametric approach: is not directly determined from the experiment but can be bounded within a plausible range.In such cases, prescribing an interpolated h(T) should be regarded as a modelling assumption or numerical regularisation rather than as a measured boundary condition.

Results: This result indicates that neglecting irradiation leads to an underestimation of the energy balance within the system and therefore to an incorrect steady-state thermal level

Plate2 Scenario 1 (6mAh)

Scenario	Model	Nominal k	Plate 2 $k-range$
Unirr.	Model-1	k(T)	173.3 @ $T = 293$ K
6 mAh		(ref. $k = 119 \pm 12$)	[108–130]
935 mAh		(ref. $k = 91 \pm 8$)	[83–99]

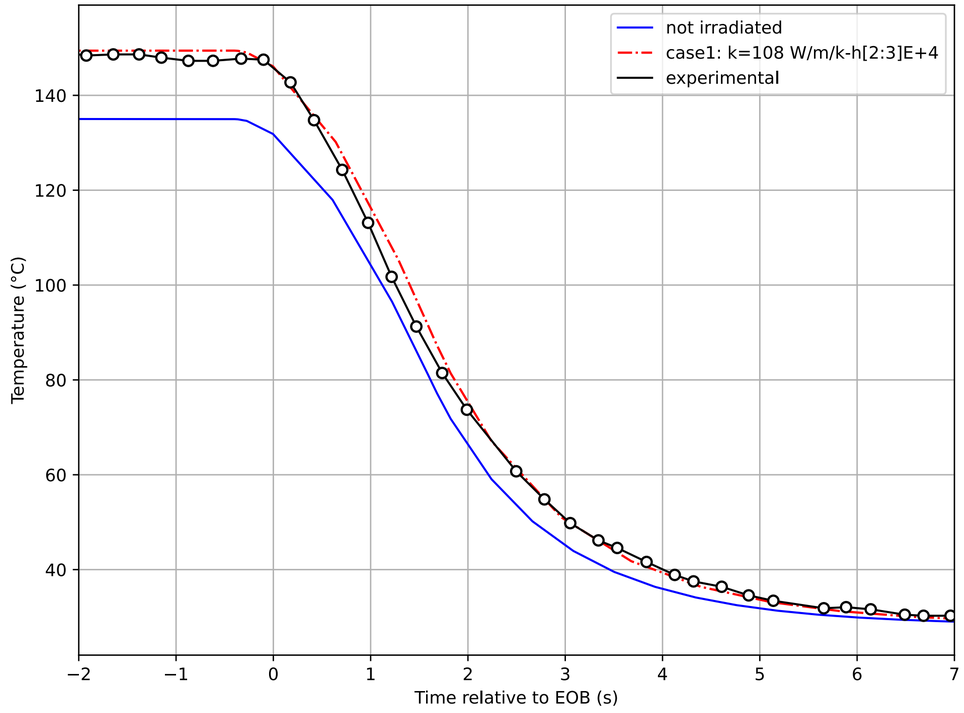

Conclusions / Future Developments

- FLUKA simulations provide predictions of DPA and gas production in the target, enabling a physics-based assessment of irradiation damage
- The k(cDPA) correlation has been used to evaluate thermal conductivity degradation and for benchmarking against experimental observations
- Overall, this work offers an independent successful check between radiation damage estimated with FLUKA and available measurements, allowing to complete the validation of the model wrt engineering parameters

AS FUTURE developments

- Improve robustness by exploring alternative and more refined k(cDPA) correlations, in collaboration with Mason et al.
- Implement advanced thermal models that explicitly account for the non-uniform spatial distribution of damage
- Couple finite element analysis (FEA) with spatially resolved DPA(x,y,z) fields derived from Monte Carlo simulations

P9 dpa spatial distribution

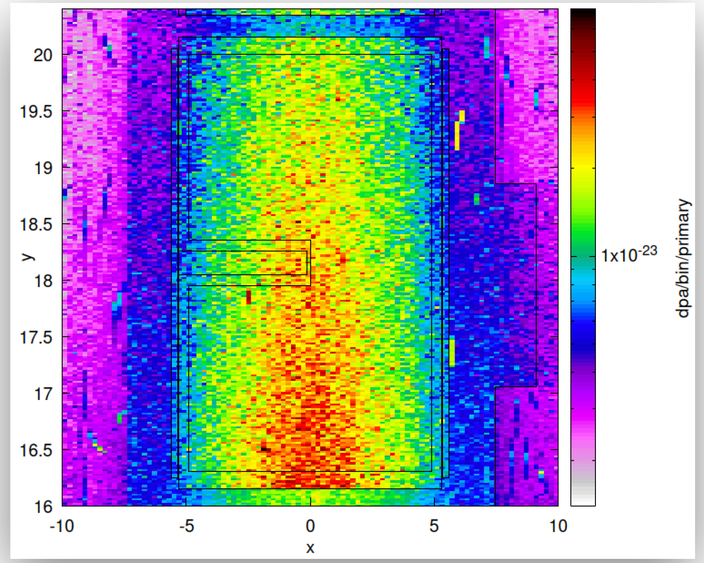

Science and Technology Facilities Council

ISIS Neutron and Muon Source

Thank you

Science and Technology Facilities Council

ISIS Neutron and Muon Source

Spares

FLUKA DPA Approach

It allows not only the characterisation of radiation fields, but also the estimation of their effects on matter

Logical sequence of process leading to radiation damage

Dislodge of Primary Knock on Atoms (PKAs)

↓

Cascade of Frenkel pairs

↓

Recombination

↓

Net displacement damage

Main source of knock-on-atoms in FLUKA—> related to a mechanism of transfer of energy

- Elastic scattering on the electrostatic potential (small deflections)
- Elastic scattering on nuclear potential (large deflections)

Not every energy transfer, T, to an atom results in a displacement.

- Damage threshold energy, E_d: only recoil energies above the threshold lead to dislodged atoms, producing a PKA

$$\mathrm{DPA}_x(E) = \frac{N_A \rho}{A_w} \int_{E_d}^{T_{\max}} dT \frac{d\sigma(E)}{dT} N_x(T_d),$$

E_d (typically 10s of eV) depending on materials

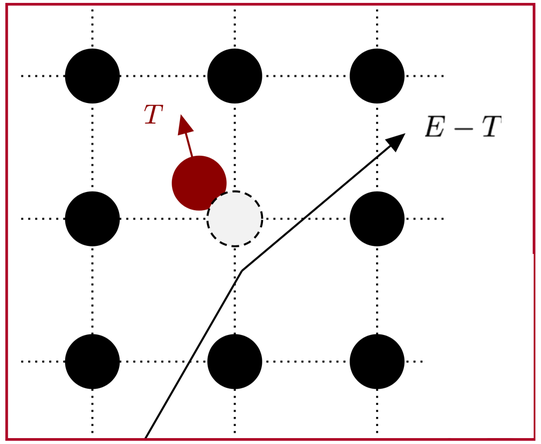

Science and Technology Facilities Council

ISIS Neutron and Muon Source

TC	ARC-DPA [dpa/pr]	
	Ni	Ta housing
1	1.3×10^{-22}	8.8×10^{-23}
2	1.2×10^{-22}	1.0×10^{-22}
3	1.4×10^{-22}	9.1×10^{-23}
4	1.1×10^{-22}	8.6×10^{-23}
5	9.0×10^{-23}	5.8×10^{-23}
6	8.0×10^{-23}	6.6×10^{-23}
7	5.2×10^{-23}	2.8×10^{-23}
8	4.4×10^{-23}	3.5×10^{-23}
9	3.3×10^{-23}	1.6×10^{-23}
10	2.0×10^{-24}	1.5×10^{-24}

The peak values in Ni is almost in the same range of peak value in W+Ta

Measured

Scenario	T_in (˚C)	T_out (˚C)	Flow (L/min)	Q_out * [kW]
6 mA·h	27.3	29.2	476	70
935 mA·h	26.8	29.0	485	82

* With an uncertainty of 20%

Simulated

Scenario	I (μA)	Prompt [MeV/pr]	Decay Heat (kW)	Q_in* (kW)
6 mA·h	134	513.562	negligible	68.9
935 mA·h	147	513.562	0.23	75.8

*With an uncertainty of 20%

Thermal diffusivity in W